Bioresource Technology 209 (2016) 228–236

Contents lists available at ScienceDirect

Bioresource Technology

journal homepage: www.elsevier.com/locate/biortech

Temperature affects microbial abundance, activity and interactions in anaerobic digestion

Qiang Lin [a,b], Jo De Vrieze [c], Jiabao Li [a], Xiangzhen Li [a,*]

[a] Key Laboratory of Environmental and Applied Microbiology, CAS, Environmental Microbiology Key Laboratory of Sichuan Province, Chengdu Institute of Biology, Chinese Academy of Sciences, Chengdu 610041, China
[b] University of Chinese Academy of Sciences, Beijing 100049, China
[c] Laboratory of Microbial Ecology and Technology, Ghent University, Coupure Links 653, B-9000 Gent, Belgium

HIGHLIGHTS

- Increased methanogenesis and hydrolysis caused high methane production.
- Increased functional orderliness with temperature enhanced methane production.
- Microbial interactions with well-defined modules are crucial for biogas digestion.

ARTICLE INFO

Article history:
Received 15 January 2016
Received in revised form 25 February 2016
Accepted 27 February 2016
Available online 3 March 2016

Keywords:
Anaerobic digestion
Temperature gradient
Community activity
Functional orderliness
Microbial interactional networks

ABSTRACT

Temperature is a major factor determining the performance of the anaerobic digestion process. The microbial abundance, activity and interactional networks were investigated under a temperature gradient from 25 °C to 55 °C through amplicon sequencing, using 16S ribosomal RNA and 16S rRNA gene-based approaches. Comparative analysis of past accumulative elements presented by 16S rRNA gene-based analysis, and the *in-situ* conditions presented by 16S rRNA-based analysis, provided new insights concerning the identification of microbial functional roles and interactions. The daily methane production and total biogas production increased with temperature up to 50 °C, but decreased at 55 °C. Increased methanogenesis and hydrolysis at 50 °C were main factors causing higher methane production which was also closely related with more well-defined methanogenic and/or related modules with comprehensive interactions and increased functional orderliness referred to more microorganisms participating in interactions. This research demonstrated the importance of evaluating functional roles and interactions of microbial community.

1. Introduction

Anaerobic digestion (AD) represents an effective process during which organic wastes, e.g. food waste and animal manure are converted into methane (Weiland, 2010). Temperature is one of important factors determining the performance and stability of the AD process (De Vrieze et al., 2015). Temperature affects AD performance through modulating microbial community composition and diversity, activities and their interactions, altering the biochemical conversion pathways and thermodynamic equilibrium of the biochemical reactions (Wilson et al., 2008). Due to different adaption potential of different microorganisms to temperature, microbial community composition and abundance will shift with the changes in temperature, which can result in a shift of both predominated methanogenic pathway and process stability (Pap et al., 2015). For example, in AD systems, importance of hydrogenotrophic methanogenesis increases as temperature shifts from 37 °C to 55 °C, which is based on the observed decrease of acetoclastic *Methanosaeta* and the increase of the hydrogenotrophic *Methanothermobacter* and *Methanoculleus* at elevated temperature (Pap et al., 2015). In addition, the phylum Firmicutes increase instead of the Bacteroidetes (Pap et al., 2015), which most likely induces changes in the functional roles of microorganisms (Tian et al., 2015). Temperature shifts the abundance and activity of specific populations, which determines the roles of specific taxa in the AD food chain including four steps: substrate hydrolysis, acidogenesis, acetogenesis, and methanogenesis. Enrichment of certain functional microorganisms at specific temperatures may be

* Corresponding author.
E-mail address: lixz@cib.ac.cn (X. Li).

http://dx.doi.org/10.1016/j.biortech.2016.02.132
0960-8524/

one of ways by which temperature affects the methane production process. Although the effects of temperature on AD performance have been investigated in many studies (Mao et al., 2015; Pap et al., 2015; Yu et al., 2014), a systematic elucidation concerning the relationship between differences in abundance and activity of specific taxa, and AD process performance, based on a comprehensive temperature gradient (25–55 °C), is still lacking.

In AD systems, overall process stability and efficiency rely on multiple syntrophic interactions among different taxa, including both bacteria and archaea. Efficient interactions among functional taxa or microbial consortia are required to sustain the process chain in AD systems to prevent accumulation of hydrogen or excessive acidification (Rui et al., 2015). As such, an AD system can be considered an artificial microbial ecosystem with high diversity and complexity. In these artificial microbial ecosystems, process chains may own classical network topology, such as modularity and small world effect (Montoya and Sole, 2002). Analysis based on network will shed light on the mechanisms regulating the interactions among microorganisms that improve AD performance. Recently, there have been several studies in which the potential organization of the microbial community in networks was investigated, such as the microbial community in the soil (Navarrete et al., 2015), marine water (Duran et al., 2015) and human intestine (Zhang et al., 2014). However, little is known about the interactions among microorganisms in AD systems under a temperature gradient, and how these interactions are regulated by temperature. Temperature can influence the reaction kinetics and thermodynamic equilibrium, which can have a substantial impact on syntrophic interactions. Phylogenetic molecular ecological networks (pMENs) based on random matrix theory tolerate noise, and create reliable and robust networks, which is important for dealing with the large-scale data with potentially high noise, such as high-throughput sequencing data (Deng et al., 2012). In contrast to common co-occurrence networks, pMENs are more powerful in discerning network interactions, including competitive and syntrophic interactions (Deng et al., 2012).

Most previous studies concerning the temperature effect on the microbial community are based on 16S rRNA gene, which detects living, dormant and dead microbes, representing the total diversity of a community, but with a lack of insight about the actual *in-situ* activity (Hugoni et al., 2013; Salter et al., 2015). Consequently, analysis based only on 16S rRNA gene is insufficient to present the actual state and composition of the microbial community in real time. For a functional system, such as the AD system, microbial composition analysis does not reveal actual system functioning which associates closely with the activity of microbial community. The RNA molecules with extreme instability and much shorter lifetime, compared to DNA, are used to indicate metabolically active microorganisms (Brettar et al., 2012). Thus, the relationship between *in-situ* activity of the microbial community and digestion performance can be explored by amplicon sequencing based on 16S ribosomal RNA (16S rRNA). Although combining the analyses based on 16S rRNA and 16S rRNA gene, respectively, has such advantages, how to explain the discrepancy and similarity between both analyses is crucial for evaluating the roles and contributions of specific populations in AD systems.

In this study, anaerobic digestion of swine manure was carried out under a temperature gradient (25–55 °C) at lab scale reactors, combining 16S rRNA and 16S rRNA gene amplicon sequencing, to investigate the response patterns of both microbial abundance and activity profiles, and interactions to changes in temperature. The main focus was placed on (i) the relationship between differences in microbial abundance and activity profiles, and AD performance, especially for methane production, (ii) discrepancy in abundance and activity of specific taxa (iii) microbial interactions under a temperature gradient.

2. Methods

2.1. Setup of biogas digestion system

For the anaerobic digestion experiment, a 2 L anaerobic flask containing 1.5 L digestion sludge with resulting total solid content of 8% was set up (Supplementary Table S1). Two holes on the upper and lower flask-wall were set for feeding and digestate removal, by a peristaltic pump (Cat. NO. BT50s, Leadfluid, China). Seed sludge of 450 mL was inoculated for each flask at the start of the experiment. To prepare, fresh swine manure had been anaerobically incubated semi-continuously under respective experimental temperature at an HRT of 30 days. Each treatment was operated for at least one time the HRT, and the digestion performance was kept at a dynamic equilibrium with biogas containing more than 60% of CH_4. The digestion temperature was set up at 25 °C, 35 °C, 45 °C, 50 °C and 55 °C, with triplicate reactors for each temperature. After first peak of daily CH_4 production (DCP) in a reactor, a semi-continuous feeding mode was operated in which 150 mL of digestate was replaced with the same volume of fresh swine manure slurry every four days. The organic loading rate was set at 2 g VS L^{-1} day^{-1}, so that a dynamic equilibrium was maintained for the fermentation process (stable period). The reactor was shaken manually twice a day. Detailed information about the parameters at the start of the experiment was shown in Supplementary Table S1.

2.2. Sampling and chemical analysis

The sludge samples were collected at peak I (the time varied based on the temperature, labeled as 25P, 35P, 45P, 50P, 55P respectively), and in the stable period (48 h after the second feed, labeled as 25S, 35S, 45S, 50S, 55S respectively) (Supplementary Table S1). The sludge samples collected in initial period (24 h after inoculation) were only for chemical analysis. The sludge was pelleted by centrifugation at 13,400*g* for 10 min at 4 °C, and immediately used for DNA and RNA extraction. The supernatant was filtered through a 0.22 μm filter (Millipore, USA), and used for chemical analysis. The volatile fatty acids (VFAs) in the supernatant were quantified by Agilent 1260 Infinity liquid chromatography system (HPLC) (Agilent Technologies, USA) equipped with a column Hi-Plex H (300 × 6.5 mm) and a differential refraction detector (RID). The mobile phase was 0.005 M H_2SO_4 with a flow rate of 0.6 mL min^{-1}. The NH_4^+-N concentration was quantified using Nessler's reagent colorimetric method (Hart et al., 1994). The biogas production was measured by water replacement method, and the water replacement equipment was set at room temperature (about 22 °C) and air pressure (about 95.86 kPa), which avoided the bias of the measured volume, caused by different temperatures and pressures. The CH_4 and H_2 content of the biogas was measured by Agilent 7890A gas chromatography system, equipped with a 3 m stainless steel column packed with Porapak Q (50/80 mesh), and a thermal conductivity detector. The injection port, column oven, and detector were operated at 100 °C, 70 °C, and 150 °C, respectively. The carrier gas was Argon with a flow rate of 30 mL min^{-1} (Li et al., 2014a). Total solid, volatile solid and COD were measured as previously described (APHA, 1981).

2.3. DNA and RNA extraction and 16S rRNA gene amplicon sequencing

Total DNA was extracted using the Ezup Column Soil DNA Purification Kit (Sangon Biotech, China). Total RNA was extracted using the RNAprep pure Cell/Bacteria Kit (TIANGEN, China). The complimentary DNA (cDNA) was synthesized by the reverse transcription kit (Thermo, USA). The 16S rRNA gene was amplified from DNA and cDNA with the universal primers 515F (5′-GTGCCAGCM

GCCGCGGTAA-3′) and 806R (5′-GGACTACHVGGGTWTCTAAT-3′) (for both bacteria and archaea) (Xu et al., 2015). Two parallel 25 μL PCR reactions were conducted, and the PCR products were pooled for purification using electrophoresis. The details concerning PCR procedure and sample preparation were described before (Li et al., 2014b). In total, 60 samples were prepared for sequencing using the Illumina Miseq platform at Environmental Genome Platform of Chengdu Institute of Biology.

2.4. Miseq sequence data analysis

The QIIME Pipeline Version 1.7.0 (http://qiime.org/tutorials/tutorial.html) was used for amplicon sequence analysis (Caporaso et al., 2010). All sequence reads were sorted based on their unique barcodes. Chimera sequences were removed using the UCHIME algorithm (Edgar et al., 2011). Sequences were clustered into operational taxonomic units (OTUs) using a 97% identity as a cutoff, and singletons were removed. Sequences were resampled to the same sequence depth (7444 reads per sample) using daisychopper.pl (http://www.festinalente.me/bioinf/downloads/daisychopper.pl) for downstream analysis. The phylogenetic affiliation of each sequence was analyzed by the Ribosomal Database Project classifier (Wang et al., 2007). The original sequencing data are available at the European Nucleotide Archive by accession no PRJEB12360 (http://www.ebi.ac.uk/ena/data/view/PRJEB12360).

2.5. Statistical analysis

The general changes of microbial community structure with temperature were evaluated by principal coordinates analysis (PCoA) and PERMANOVA performed with R (http://www.r-project.org/) based on the Bray–Curtis distance. The similarity between microbial communities based on the 16S rRNA and 16S rRNA gene datasets was also assessed based on Bray–Curtis distance. The normality and homoscedasticity of the data were evaluated in SPSS 21 software (IBM, USA). One-way-analysis of variance (ANOVA) performed in SPSS 21 software was used to test the differences in relative abundances of taxonomic units between samples from different temperatures. Pearson's correlation analysis was performed in *R* to assess the correlation between variables. Regression analysis was conducted using OriginPro 8.5 software (OriginLab USA). A computational approach, phylogenetic investigation of communities by reconstruction of unobserved states (PICRUSt) (Langille et al., 2013), was used to predict functional profiles of a microbial community in the AD system, using both 16S rRNA gene and 16S rRNA datasets. Due to universality of KEGG database, it was chosen for functional predictions, and the pathway hierarchy level 3 was chosen as output. Enrichment analysis was conducted by combining Fisher's exact test in *R* and independent-samples *T* test in the SPSS 21 software.

Random matrix theory-based phylogenetic molecular ecological networks (pMENs) were constructed as described before (Deng et al., 2012). The PMENsR and pMENsD were constructed based on the 16S rRNA and 16S rRNA gene-based analysis, respectively, in which OTUs with an occurrence in less than three samples were excluded. Significant differences between these two pMENs and their corresponding random networks with identical network sizes in terms of modularity, average clustering coefficient, and average geodesic distance (Supplementary Table S5), ensured that both these two pMENs constructed possessed typical small world modularity and hierarchy properties (Deng et al., 2012). The topological roles of nodes could be classified into four subcategories based on the values of *Zi* and *Pi*: peripheral nodes ($Zi \leqslant 2.5$, $Pi \leqslant 0.62$), connectors ($Zi \leqslant 2.5$, $Pi > 0.62$), module hubs ($Zi > 2.5$, $Pi \leqslant 0.62$) and network hubs ($Zi > 2.5$, $Pi > 0.62$) (Supplementary Fig. S7) (Deng et al., 2012).

3. Results and discussion

3.1. Digester performance

3.1.1. Biogas production

The time at which the first peak of daily CH_4 production (DCP) varied with temperature (Fig. S1a). The first peak was highest at 50 °C (1.9 L L^{-1} d^{-1}), while it was lowest at 25 °C (0.4 L L^{-1} d^{-1}) (Fig. 1). After the first peak, the DCP showed a dynamic equilibrium until the end of the experiments. Although the DCPs in the first peak and stable period showed certain differences at specific temperatures, both of them reflected the similar pattern along the temperature gradient (Fig. 1). The DCP increased from 25 °C to 50 °C, but decreased at 55 °C. Total biogas production over a period of 27 days increased with temperature from 25 °C to 50 °C, but decreased at 55 °C (Fig. S1c). The CH_4 content in the biogas increased with temperature from 25 °C to 45 °C, and was stable at higher temperature, around 60% CH_4 content during the stable period (Supplementary Fig. S1b). The H_2 content in the biogas remained between 0.1% and 0.8% during the entire experiment. Because the DCP and total biogas production showed the same changing patterns with temperature, the DCP was considered as an indicator of fermentation performance in this study for further analysis.

3.1.2. VFAs dynamics

Acetic acid, propionic acid and butyric acid were detected as main VFAs under various temperatures (Supplementary Fig. S2). Acetic acid concentration decreased over time, and remained at 2–4 mM during the stable period at all temperatures. The changes in butyric acid and propionic acid showed a similar pattern with that of acetic acid from 35 °C to 55 °C. At 25 °C, butyric acid and propionic acid accumulated up to 37 mM and 22 mM, respectively. The conversion rates of VFAs were highest at 50 °C, and lowest at 25 °C. Total VFAs in the peak and stable periods showed a clear difference along the temperature gradient (Supplementary Fig. S2d), indicating that fermentation conditions varied at different temperatures. The VFAs concentrations showed negative correlations with DCP ($p < 0.01$) (Supplementary Table S2).

The pH value was 7.0 at beginning, and gradually increased until the stable period (7.4–7.8) at different temperatures. The NH_4^+-N concentration increased slightly and was kept stable (320–780 mg L^{-1}) throughout the process.

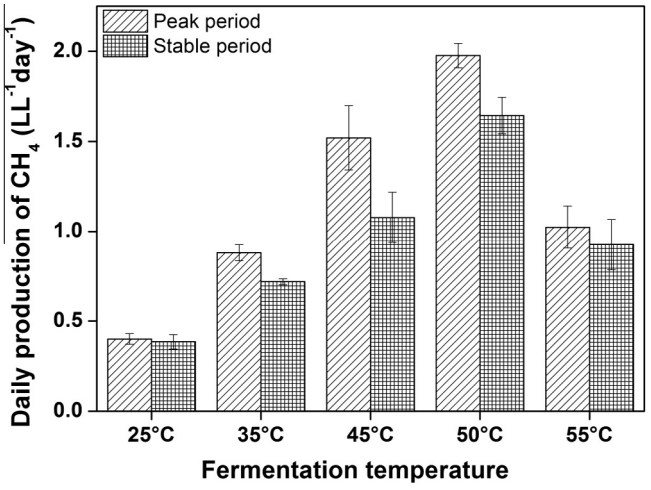

Fig. 1. Daily CH_4 production in the peak and stable period. All the data are presented as means ± standard deviations ($n = 3$).

3.2. Microbial community composition analysis

3.2.1. Variation of microbial community structure

Principal coordinates analysis (PCoA) and PERMANOVA tests showed significant differences ($p < 0.001$) of the microbial community along temperature gradient, based on both the 16S rRNA gene ($R^2 = 0.43$) and 16S rRNA ($R^2 = 0.62$) analysis (Fig. 2). The samples from each specific temperature formed a cluster, thus, combining samples in both the peak and stable period was suitable to reveal the relationship between microbial community and fermentation performance at different temperatures for further analysis. The variation of microbial community did show a similar pattern, based on both 16S rRNA and 16S rRNA gene analysis along the temperature gradient.

3.2.2. Comparison of microbial community composition and activity between 25 °C and 50 °C

A clear shift of the microbial community abundance (16S rRNA gene) and activity (16S rRNA) was observed along the different temperatures. Enrichment analysis was conducted to further reveal the differences. The comparison between the 25 °C and 50 °C treatment was selected, as they showed poorest and best performance, respectively.

There were 195 and 90 OTUs significantly enriched at 50 °C and 25 °C, respectively, based on the 16S rRNA gene dataset (Supplementary Fig. S3). Among the main OTUs enriched at 50 °C (Table 1), OTU84 affiliated to *Ruminofilibacter xylanolyticum* which is responsible for the degradation of xylan (Weiss et al., 2011) with relative abundance of 5.92% compared to 0.49% at 25 °C, and OTU135 (*Porphyromonadaceae*) with a 22-fold enrichment were affiliated to the phylum Bacteroidetes, while other OTUs were mainly affiliated to the phylum Firmicutes and Thermotogae. Except for OTU171 (affiliated to candidate genus S1 in Phylum Thermotogae), all other OTUs enriched at 50 °C showed positive correlations ($p < 0.01$) with DCP over the entire temperature gradient (Table 1). The candidate genus S1 may produce metabolic intermediates that can be used by methanogens (Maus et al., 2015). At 25 °C, both OTU10553 (8.5%) and OTU5 (4.8%), affiliated to the genus *Prevotella*, negatively correlated with temperature and DCP ($p < 0.01$), but positively correlated with VFAs ($p < 0.01$).

In the 16S rRNA datasets, there were 157 and 202 OTUs enriched at 50 °C and 25 °C, respectively (Supplementary Fig. S3). Among the main OTUs enriched at 50 °C (Table 1), OTU183 affiliated to *Lactobacillus* which is responsible for lactic acid production in the acidogenesis stage (De Vrieze et al., 2015) and OTU84 with a relative abundance of 7.7% and 5.4%, respectively, showed positive correlation with DCP ($p < 0.01$), but negative correlation with certain VFAs ($p < 0.05$) during the entire temperature gradient (25–55 °C). The OTU7621, 5360, 7743 and 9709 (all affiliated to *Methanosarcina*) and OTU391 (*Pseudomonadaceae*) also positively correlated with DCP ($p < 0.05$) during the entire temperature gradient. Among the main OTUs enriched at 25 °C, only OTU764 (*Methanofollis*) was affiliated to the methanogens, but showed negative correlation ($p < 0.01$) with both DCP and temperature over the entire temperature gradient.

At order and genus level, similar enrichment patterns were detected compared to that at OTU level (Supplementary Fig. S4). There were more orders referred to hydrolysis and methanogenesis enriched at 50 °C compared to 25 °C. At genus level, taxa such as *Ruminofilibacter*, *Lactobacillus*, *Methanosarcina*, and candidate genus S1 were enriched at 50 °C compared to 25 °C where *Prevotella* and *Bacteroides* were mainly enriched. Both *Bacteroides* and *Prevotella* are able to degrade cellulose and xylan, proteins and peptides (Hatamoto et al., 2014; Wallace et al., 1997). Interestingly, although in general the specific taxa based on 16S rRNA gene and rRNA datasets showed similar enriched patterns between different temperatures, the relative abundances of specific taxa based on 16S rRNA gene and 16S rRNA datasets were different. In addition, the whole activities of microbial community are assessed by the similarity of the microbial community between 16S rRNA gene and 16S rRNA-based analysis (Brettar et al., 2012). The similarity was 0.20 ± 0.01 and 0.42 ± 0.01 at 25 °C and 50 °C, respectively, indicating that more present OTUs were active and might perform their specific biogeochemical functions at 50 °C than that at 25 °C.

PICRUSt predictions based on both the 16S rRNA gene and 16S rRNA were carried out for further comparison of the function profiles (Supplementary Table S3). At the KEGG level 3, among the abundant predicted pathways, methane metabolism (Ko00680, mainly referred to methanogenesis in AD systems), Two-component system (Ko02020) which accelerates cellular response to external stimuli usually by inducing changes in transcription (Yamamoto et al., 2005), and bacterial motility proteins (Ko02035), which improve spontaneous cell movement to resource locations (Marisch et al., 2013) for efficient resource utilization, were enriched at 50 °C, based on both the 16S rRNA gene and 16S rRNA datasets, and positively correlated with temperature and DCP ($p < 0.01$). DNA repair and recombination proteins (Ko03400) were enriched at 25 °C with highest enrichment fold (about 1.1).

3.2.3. Microbial community composition and activity comparison between 50 °C and 55 °C

There were fewer OTUs whose relative abundances changed significantly between 50 °C and 55 °C than between 25 °C and

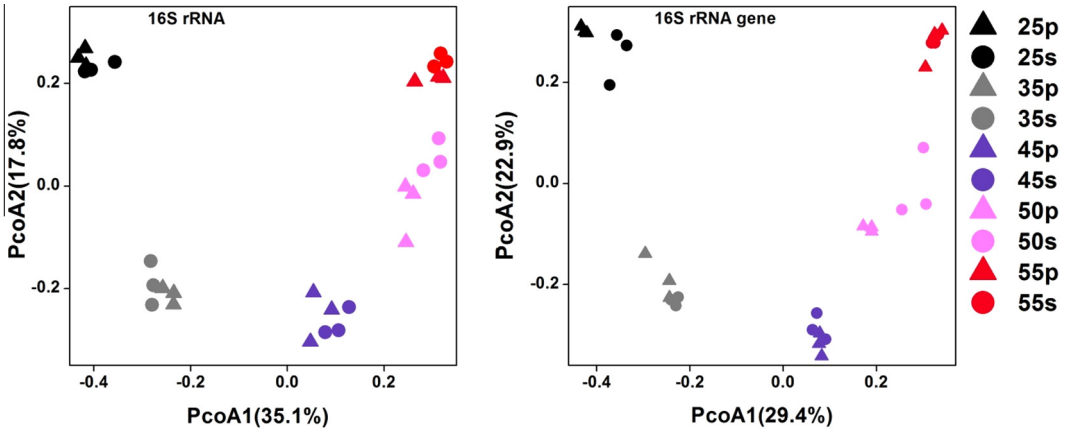

Fig. 2. The principal coordinates analysis based on the entire microbial community at different temperatures. "P" and "S" stand for peak and stable period, respectively; the numbers mean temperature.

Table 1
Relative abundance profiles of main OTUs and correlations by comparison between 25 °C and 50 °C, based on 16S rRNA gene and 16S rRNA datasets. Only enriched taxa with an average relative abundance >1% are shown.

16S rRNA gene	Average relative abundance (%)		Enrichment fold				Correlation during entire temperature gradient (25–55 °C)					
OTU ID	25 °C	50 °C	25 °C	50 °C	Phylum	Affiliation	Temperature	DCP	Acetate	Propionate	Butyrate	pH
OTU10553	8.501	0.025	340.04		Bacteroidetes	*Prevotella*	−.692**	−.581**	.805**	.617**	.854**	−.868**
OTU5	4.798	0.027	177.704		Bacteroidetes	*Prevotella*	−.692**	−.586**	.753**	.623**	.857**	−.838**
OTU28	2.796	0.043	65.023		Firmicutes	*Lachnospiraceae*	−.760**	−.653**	.546**	.779**	.952**	−.792**
OTU8888	1.961	0.011	178.273		Firmicutes	*Clostridiales*	−.739**	−.644**	.363*	.806**	.919**	−.655**
OTU11250	1.914	0.058	33		Firmicutes	*Anaerostipes*	−.694**	−.563**	.796**	.649**	.852**	−.878**
OTU51	1.715	0.036	47.639		Bacteroidetes	YRC22	−.485**	−.386*	.182	.089	.057	−.199
OTU8996	1.426	0.009	158.444		Firmicutes	*Anaerostipes*	−.697**	−.588**	.724**	.664**	.869**	−.851**
OTU8866	1.334	0.004	333.5		Firmicutes	*Lachnospiraceae*	−.688**	−.591**	.656**	.650**	.859**	−.801**
OTU762	1.316	0.002	658		Bacteroidetes	*Bacteroides*	−.649**	−.564**	.531**	.678**	.813**	−.700**
OTU3563	1.225	0.02	61.25		Bacteroidetes	*Prevotella*	−.685**	−.592**	.459*	.712**	.849**	−.674**
OTU10434	1.214	0.002	607		Firmicutes	*Lachnospiraceae*	−.645**	−.538**	.840**	.559**	.802**	−.870**
OTU84	0.49	5.92		12.082	Bacteroidetes	*Ruminofilibacter xylanolyticum*	.373*	.611**	−.306	−.136	−.464**	.177
OTU5171	0.076	2.136		28.105	Thermotogae	S1	.729**	.205	−.179	−.649**	−.379*	.521**
OTU8354	0.063	1.948		30.921	Firmicutes	*Clostridiales*	.537**	.869**	−.284	−.508**	−.420*	.342
OTU4820	0.116	1.905		16.422	Firmicutes	*Clostridium*	.373*	.662**	−.187	−.158	−.307	.141
OTU6720	0.027	1.328		49.185	Firmicutes	*Clostridiales*	.566**	.870**	−.315	−.493**	−.445*	.384*
OTU135	0.054	1.162		21.519	Bacteroidetes	*Porphyromonadaceae*	.608**	.634**	−.260	−.337	−.477**	.384*
OTU4187	0.139	1.081		7.777	Firmicutes	*Sedimentibacter*	.275	.695**	−.235	−.104	−.342	.150
16S rRNA OTU ID												
OTU23	3.889	0.027	144.037		N	Bacteria	−.732**	−.635**	.520**	.737**	.919**	−.774**
OTU327	2.172	0.038	57.158		Bacteroidetes	*Rikenellaceae*	−.752**	−.634**	.744**	.735**	.942**	−.871**
OTU161	2.002	0.02	100.1		Bacteroidetes	*Rikenellaceae*	−.777**	−.667**	.611**	.796**	.971**	−.823**
OTU104	1.858	0.018	103.222		Bacteroidetes	*Bacteroides*	−.647**	−.535**	.869**	.568**	.807**	−.885**
OTU2018	1.693	0.246	6.882		WWE1	W22	−.278	−.071	−.051	.240	−.147	−.115
OTU764	1.643	0.051	32.216		Euryarchaeota	*Methanofollis*	−.594**	−.501**	.097	.547**	.458*	−.393*
OTU152	1.464	0.219	6.685		WWE1	W22	−.304	−.095	−.058	.250	−.149	−.114
OTU96	1.296	0.004	324		Firmicutes	*Clostridiales*	−.755**	−.670**	.284	.851**	.947**	−.635**
OTU248	1.046	0.034	30.765		N	Bacteria	−.821**	−.705**	.353	.858**	.924**	−.645**
OTU183	1.274	7.733		6.07	Firmicutes	*Lactobacillus*	.808**	.591**	−.242	−.666**	−.492**	.520**
OTU84	0.381	5.38		14.135	Bacteroidetes	*Ruminofilibacter xylanolyticum*	.241	.556**	−.252	−.085	−.417*	.140
OTU1848	0.596	2.328		3.91	Euryarchaeota	*Methanoculleus*	.418*	.265	−.318	−.618**	−.509**	.453*
OTU7621	0.076	1.805		23.706	Euryarchaeota	*Methanosarcina*	.768**	.551**	−.256	−.681**	−.451*	.545**
OTU5360	0.054	1.791		33.333	Euryarchaeota	*Methanosarcina*	.723**	.625**	−.244	−.645**	−.442*	.498**
OTU5171	0.051	1.52		29.522	Thermotogae	S1	.690**	.151	−.167	−.593**	−.364*	.475**
OTU10334	0.083	1.489		17.973	Thermotogae	S1	.679**	.129	−.172	−.576**	−.360	.483**
OTU7743	0.056	1.196		21.36	Euryarchaeota	*Methanosarcina*	.784**	.584**	−.257	−.693**	−.462*	.557**
OTU9709	0.016	1.043		66.571	Euryarchaeota	*Methanosarcina*	.644**	.436*	−.211	−.578**	−.375*	.447*
OTU391	0.215	1.023		4.76	Proteobacteria	*Pseudomonadaceae*	.401*	.413*	−.214	−.349	−.316	.384*

"N" means unclassified.
* Significant at $p < 0.05$.
** Significant at $p < 0.01$.

50 °C (Table 2). Although OTU15671 (*Methanobacterium*) was enriched at 55 °C, it showed no significant correlation with DCP during the entire temperature gradient (25–55 °C), indicating its limited contributions to methanogenesis in the AD system. The predict function profiles of PICRUSt also showed no significant difference in methane metabolism between 50 °C and 55 °C (Supplementary Table S4). Instead, digesters with OTUs affiliated to the orders *Clostridiales* and *Bacteroidales*, especially OTU84 were more abundant at 50 °C compared to that at 55 °C, which provided more potential for substrate degradation (Supplementary Fig. S5). The predict function profiles also showed more pathways referred to the degradation of organic substrates, such as arginine, proline and pyruvate, at 50 °C compared to those at 55 °C (Supplementary Table S4).

3.2.4. The relationship between digestion performance and abundance profiles of the microbial community

Each step in the AD process is carried out by different microbial consortia in which each microorganism owns a specific ecological niche in the AD system (Zhang et al., 2015). The changes in environmental variables, such as temperature, pH and resource limitation, cause changes in species composition. Although in general the microbial community based on 16S rRNA and 16S rRNA gene datasets reflected similar differentiation pattern under the temperature gradient, some specific taxa showed significantly different relative abundances and activities based on the 16S rRNA gene and 16S rRNA datasets, respectively, even at same temperature. Explaining the differences in abundance and activity of specific taxa could further evaluate the roles and contributions of specific taxa in the AD system, and the discrepancies in methane production under temperature gradient can be explained.

Analysis of the 16S rRNA gene reflects the abundance of taxa, in spite of their activity in the metabolic process, which merely indicates the actual spatial existence of taxa in AD systems. However, the 16S rRNA is used to indicate metabolically active microorganisms (Brettar et al., 2012; Hugoni et al., 2013), which indicates actual participation in the AD process. Based on above viewpoints, the assumptions were made that (i) spatial ecological niches are defined based on 16S rRNA gene, which indicates the actual spatial existence in the form of cellular quantities; (ii) functional ecologi-

Table 2
Relative abundance profiles of main OTUs and correlations by comparison between 50 °C and 55 °C, based on 16S rRNA gene and 16S rRNA datasets. Only enriched taxa with average relative abundances >1% are shown.

16S rRNA gene	Average relative abundance (%)		Enrichment fold				Correlation during entire temperature gradient (25–55 °C)					
OTU ID	50 °C	55 °C	50 °C	55 °C	Phylum	Affiliation	Temperature	DCP	Acetate	Propionate	Butyrate	pH
OTU84	5.92	0.313	18.914		Bacteroidetes	*Ruminofilibacter xylanolyticum*	.187	.611**	−.306	−.136	−.464**	.177
OTU8354	1.948	0.367	5.308		Firmicutes	*Clostridiales*	.537**	.869**	−.284	−.508**	−.420*	.342
OTU4820	1.905	0.472	4.036		Firmicutes	*Clostridium*	.373*	.662**	−.187	−.158	−.307	.141
OTU6720	1.328	0.291	4.564		Firmicutes	*Clostridiales*	.566**	.870**	−.315	−.493**	−.445*	.384*
OTU4187	1.081	0.056	19.304		Firmicutes	*Sedimentibacter*	.275	.695**	−.235	−.104	−.342	.150
OTU10334	2.165	7.055		3.259	Thermotogae	S1	.688**	.131	−.156	−.606**	−.350	.475**
OTU5171	2.136	5.273		2.469	Thermotogae	S1	.729**	.205	−.179	−.649**	−.379*	.521**
OTU1955	0.132	3.838		29.076	Firmicutes	*Clostridiales*	.562**	−.107	−.089	−.447*	−.260	.368*
OTU11745	0.587	2.25		3.833	Thermotogae	S1	.676**	.097	−.151	−.589**	−.340	.478**
OTU1156	0.318	1.711		5.381	N	Bacteria	.674**	.020	−.128	−.559**	−.333	.456*
OTU4500	0.419	1.558		3.718	Thermotogae	S1	.687**	.095	−.162	−.601**	−.350	.512**
OTU3823	0.363	1.493		4.113	Thermotogae	S1	.697**	.069	−.150	−.588**	−.346	.484**
OTU9631	0.432	1.46		3.38	Thermotogae	S1	.698**	.122	−.163	−.616**	−.357	.484**
OTU14528	0.193	1.037		5.373	Thermotogae	S1	.657**	.043	−.142	−.557**	−.330	.502**
16S rRNA OTU ID												
OTU84	5.38	1.048	5.135		Bacteroidetes	*Ruminofilibacter xylanolyticum*	.241	.556**	−.252	−.085	−.417*	.140
OTU10334	1.489	4.455		2.992	Thermotogae	S1	.679**	.129	−.172	−.576**	−.360	.483**
OTU5171	1.52	4.348		2.86	Thermotogae	S1	.690**	.151	−.167	−.593**	−.364*	.475**
OTU15671	0.403	1.482		3.678	Euryarchaeota	*Methanobacterium*	.639**	.094	−.143	−.562**	−.322	.519**
OTU11745	0.325	1.124		3.462	Thermotogae	S1	.664**	.118	−.152	−.556**	−.345	.446*

"N" means unclassified.
* Significant at $p < 0.05$.
** Significant at $p < 0.01$.

cal niches are defined based on 16S rRNA, which indicates the actual roles in the metabolic process in the form of cellular activities. For example, the OTU10553 (*Prevotella*) was abundant (8.5%) based on 16S rRNA gene datasets, but rare (0.5%) based on 16S rRNA datasets at 25 °C, which indicated that OTU10553 played more important roles in spatial ecological niche than functional ecological niche. This phenomenon could be explained by the initial input of swine manure (Marti et al., 2011) or rapid proliferation in the initial stage of the fermentation. The cellular quantities of OTU10553 increased strongly, but the metabolic activity and/or growth rate gradually slowed down as fermentation proceeded, probably due to an increased competition, accumulation of metabolic intermediates and/or resource limitation (Campbell et al., 2011). Thus, taxa like OTU10553 were considered in an inactive condition when fermentation process was in the peak and stable period, which caused their limited contribution to methane production, especially in the stable period. If the accumulation of metabolic intermediates played a stronger role in the decrease of the metabolic activity of OTU10553, a slow turnover of metabolic intermediates could be indicated at 25 °C, which was also supported by slow conversion of VFAs at 25 °C.

The OTU7621 (*Methanosarcina*) was rare (0.4%) based on 16S rRNA gene datasets but abundant (1.8%) based on 16S rRNA datasets at 50 °C, implicating that after adaption to the environment and substrates produced by fermentative microorganisms, the metabolic activity and/or growth rate of OTU7621 was gradually enhanced. Thus, taxa like OTU7621 were in an active condition, and would gradually occupy spatial ecological niches, besides functional ecological niches. Finally, OTU84 (*R. xylanolyticum*) was abundant based on both 16S rRNA and 16S rRNA gene datasets at 50 °C, implicating that this OTU maintained high competitiveness in spatial and functional ecological niches, thus, it contributed significantly to digestion at 50 °C.

By further integrating the results of the enrichment analysis, we could reveal the reasons inducing the differences of methane production under a temperature gradient. Fermentative microorganisms, such as *Lactobacillus*, *R. xylanolyticum* and S1, and methanogens predominated by *Methanosarcina*, occupied spatial and/or functional ecological niches. Hence, nearly all the four steps, especially methanogenesis, in the AD process were strengthened at 50 °C, compared to 25 °C, which resulted in higher methane production at 50 °C. This was also supported by the results of PICRUSt prediction. In the same way, the discrepancy in methane production between 50 °C and 55 °C was mainly induced by higher hydrolysis activity at 50 °C, conducted mainly by fermentative microorganisms, e.g. *R. xylanolyticum*.

Consequently, the spatial ecological niche only shows the already existing condition, mainly referring to past cellular activities, i.e. past accumulative elements, but the functional ecological niche reflects the current active condition, which is much closely related with *in-situ* process performance. Although more data are needed to verify the definition of spatial and functional ecological niche, it provides new insights into the comprehensive understanding of the roles of specific taxa, by combining past elements and present conditions. It also supplies brand-new views on the interactions and functioning of microbial consortia.

3.3. Microbial interactions

3.3.1. General properties of molecular ecological networks of microbial communities

Phylogenetic molecular ecological networks (pMENs) (Deng et al., 2012) were constructed to reveal the interactions of the microbial community in response to changes in temperature (Fig. 3). The composition of pMENsD and pMENsR strongly differed, supported by the fact that only 110 nodes (OTUs) were

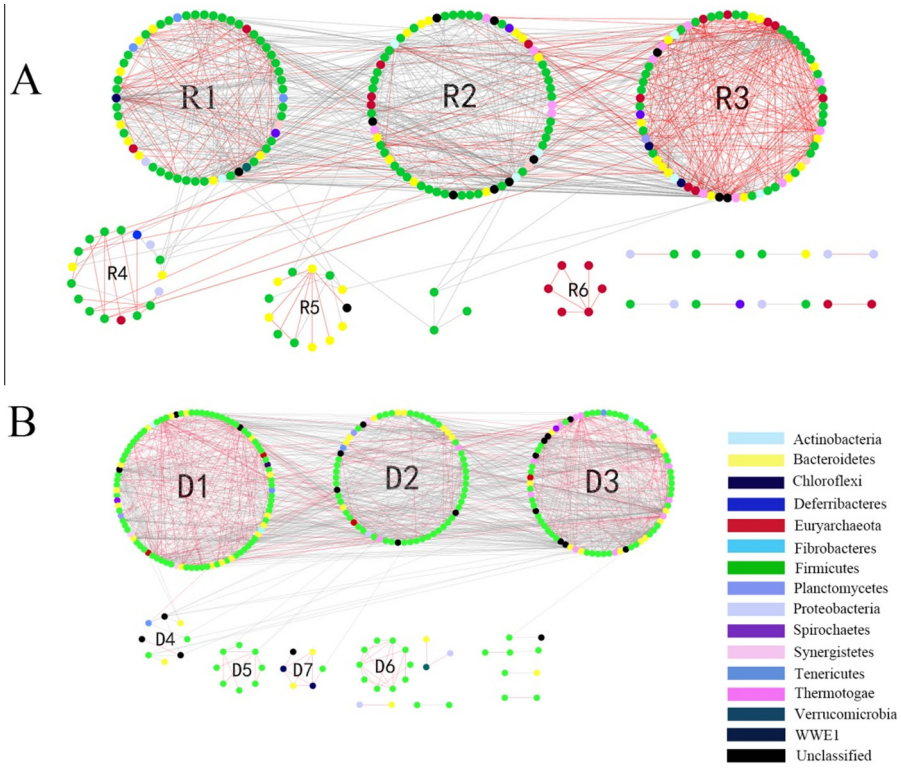

Fig. 3. Phylogenetic molecular ecological networks (pMENs) of the microbial community based on dataset of 16S rRNA (A) and 16S rRNA gene (B) over the entire temperature gradient (25–55 °C). The number in the circles represents the module number. Red lines represent positive correlations, and gray lines negative correlations.

shared between pMENsR (total 251 nodes) and pMENsD (total 270 nodes). The PMENsD had a larger size, as evaluated by number of nodes and links, than the pMENsR, but the complexity evaluated by average degree of networks (Deng et al., 2012), was higher in pMENsR (Supplementary Table S5). The accumulated relative abundances of OTUs involved in both pMENsR and pMENsD showed positive correlation ($p < 0.01$) with temperature (Fig. 4), indicating that as temperature increased, more microorganisms in the microbial community participated in interactions. As we know, in AD systems, different microorganisms perform various metabolic functions, and the microbial interactions indicate the potential connections between their metabolic functions. Hence, more microorganisms participating in interactions reflecting more various microorganisms with ordered organization (defined as orderliness), probably improves the well-organized connections between metabolic functions of microbial community. High orderliness may prevent waste and chaos of resource utilization. In complex but functionally enriched systems, such as AD systems for biogas production, an oriented and efficient conversion of the organic waste to methane is preferred. Thus, more various taxa with ordered organization would result in efficient utilization of resources and prevention of a potential system crash.

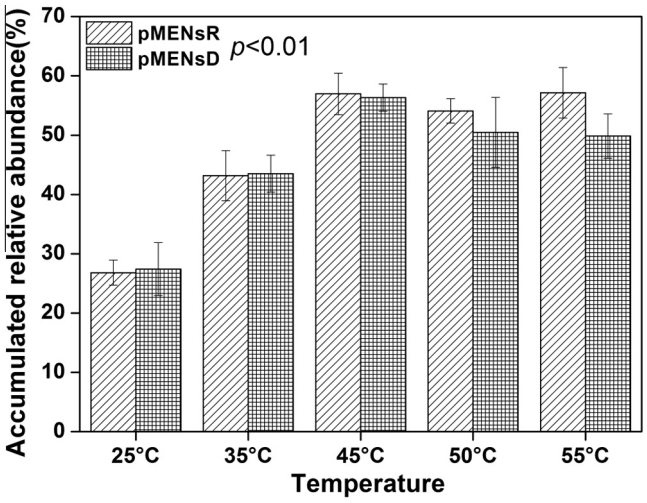

Fig. 4. The accumulated relative abundances of OTUs involved in pMENsR and pMENsD assessed under the temperature gradient (25–55 °C). Both accumulated relative abundances showed a positive correlation ($p < 0.01$) with temperature.

3.3.2. Module analysis of pMENs

In the pMENs, a module is considered a group of OTUs that share similar ecological niches, and performs a similar or complementary function in a given system (Deng et al., 2012). In this study, there were 6 modules in pMENsR and 7 in pMENsD. The responses of the modules to changes in environment and function in the AD systems were detected from the correlations between module-based eigengenes and environmental factors. In pMENsR, the modules R1, R2, R3 and R5 showed a significant positive correlation with DCP ($p < 0.001$), but negative correlation with the concentrations of several VFAs (Fig. 5). Only modules R1, R2 and R3 significantly and positively correlated with temperature. In pMENsD, the modules D1, D2 and D5 showed a significant positive correlation with DCP and temperature, but negative correlation with the concentrations of several VFAs (Fig. 5).

The function of each module in pMENs can be derived from the microbial composition and their known physiological functions, and PICRUSt prediction (Rui et al., 2015). The module R1, mainly composed of Firmicutes (65.5%) and Bacteroidetes (13.8%) (Supplementary Table S6), was predicted to conduct fermentation. The R3 was the methanogenic module, dominated by *Methanosarcina*. The R5 was also a fermentation module, dominated by *R. xylanolyticum*. Inside the modules R1 and R5, around 40% and 62% positive corre-

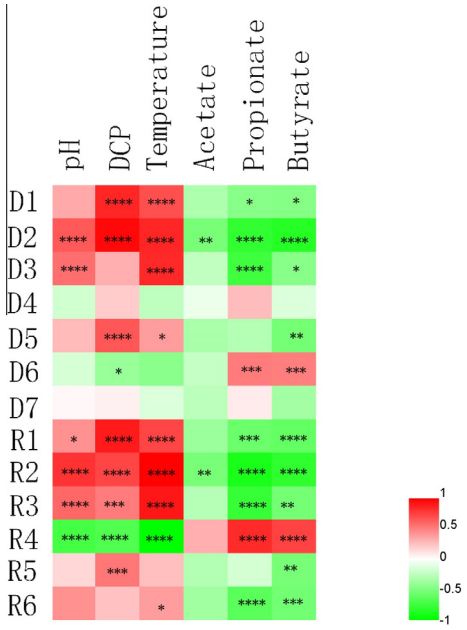

Fig. 5. The correlations between module-based eigengenes and environmental factors in pMENs. **** Significant at $p < 0.0001$, *** significant at $p < 0.001$, ** significant at $p < 0.01$, * significant at $p < 0.05$.

lations were observed, but they showed negative correlation with the nodes outside, implicating a cooperation relationship between OTUs inside these modules, while more competition between different modules (Fig. 3). In contrast, the methanogenic module R3 showed a clear cooperation relationship with other modules, and the nodes inside R3 also showed positive correlation with each other. This supported that methane production requires comprehensive cooperation between methanogens and other fermentative microorganisms. The R6 was completely composed of methanogens, and was assumed to conduct methanogenesis, but showed no significant correlation with DCP, which might be explained by the topological roles that R6 showed no interactions with other modules.

Variance partitioning analysis was performed to quantify the relative contributions of the different modules to DCP (Supplementary Fig. S6). The R1 alone explained 10%, R2 1%, R3 13% and R5 11% of total variation, leaving 26% of the variation unexplained, while above modules together explained 34% of total variation. The functions of these four modules were also related to the topological roles of nodes in these modules (Supplementary Fig. S6). As module hubs, OTU12948 (*Clostridia*), OTU7621 (*Methanosarcina*), OTU7835 (*Clostridiales*) and OTU84 (*R. xylanolyticum*) showed positive correlation with DCP ($p < 0.05$) (Supplementary Table S7). Overall, OTU12948 showed positive correlation with the OTUs affiliated to the class *Clostridia,* but negative correlation with the OTUs affiliated to the phylum Bacteroidetes and the genus *Fibrobacter* in the pMENsR (Supplementary Table S8). The OTU7621 showed positive correlation with several fermentative microorganisms, implicating that methanogenesis required the cooperation between methanogens and fermentative microorganisms in AD systems. This was further supported by the fact that R6 which consisted of methanogens, without interactions with other modules, showed no significant contribution to methane production. As another module hub in R3, OTU7835 showed negative correlation with the OTUs affiliated to the phylum Bacteroidetes and the genus *Fibrobacter*, which indicated the competition between them. All the correlations between the OTU84 and the other OTUs were positive, which reflected a high degree of cooperation.

In pMENsD, the modules D1, D2 and D5, showed significant positive correlation with DCP. They mainly performed hydrolysis, acidogenesis and acetogenesis in AD systems, based on the composition of these modules (Supplementary Table S9). Inside the modules of D1 and D5, around 36% and 100% positive correlations were observed, indicating the cooperation existence within these modules (Fig. 3). However, overall, comprehensive negative correlation occurred among the modules in pMENsD. In the variance partitioning analysis, the D1 alone explained 11%, D2 14%, and D5 0.2% of total variation, leaving 29% of the variation unexplained, while above modules together explained 42% of total variation (Supplementary Fig. S8). Given topological roles of nodes in networks, there were more module hubs but fewer connectors and network hubs in pMENsD compared to pMENsR (Supplementary Fig. S7, Tables S9 and S12). This implicated fewer interactions between the modules in pMENsD than those in pMENsR, which corresponded well to respective complexity of these two pMENs.

Overall, pMENsD and pMENsR clearly reflected different interaction states generally evaluated by network properties and shared OTUs. The differences were induced by past accumulative elements and present conditions in the AD system. First, in pMENsR, a higher complexity of networks implies higher connectivity (Deng et al., 2012), which provided more functional redundancy. Second, there were more well-defined functional modules in pMENsR reflecting the fine orderliness and organization of microbial community. Finally, topological roles of nodes in pMENsR, with more connectors and network hubs, indicated more interactions among microorganisms to improve the efficiency of the process. Although the two pMENs clearly reflected different interaction states, both of them demonstrated increased functional orderliness and well-defined modules along a temperature gradient, which indicated the importance of temperature to regulate the microbial interactions.

4. Conclusions

This study introduced concepts of past accumulative elements (16S rRNA gene) and current conditions (16S rRNA) to evaluate functional roles of specific microbial populations, based on which the differences in methane production were revealed in the AD system under a temperature gradient. Increased methanogenesis and hydrolysis at 50 °C resulted in highest methane production. Meanwhile temperature also affected the microbial interactions mainly referred to the construction of well-defined functional modules and the functional orderliness of AD process. More well-defined methanogenic and/or related modules with comprehensive interactions and increased functional orderliness improved the efficiency of methane production.

Competing interest

Authors declare that they have no competing interests.

Acknowledgements

This work is supported by National Key Technology Support Program (2014BAD02B04) and 973 Project (No. 2013CB733502). Jo De Vrieze is supported as a postdoctoral fellow from the Research Foundation Flanders (FWO-Vlaanderen).

Appendix A. Supplementary data

Supplementary data associated with this article can be found, in the online version, at http://dx.doi.org/10.1016/j.biortech.2016.02.132.

References

APHA, 1981. Standard Methods for the Examination of Water and Wastewater, 15th ed. APHA American Public Health Association.

Brettar, I., Christen, R., Hofle, M.G., 2012. Analysis of bacterial core communities in the central Baltic by comparative RNA-DNA-based fingerprinting provides links to structure-function relationships. ISME J. 6 (1), 195–212.

Campbell, B.J., Yu, L.Y., Heidelberg, J.F., Kirchman, D.L., 2011. Activity of abundant and rare bacteria in a coastal ocean. Proc. Natl. Acad. Sci. USA 108 (31), 12776–12781.

Caporaso, J.G., Kuczynski, J., Stombaugh, J., Bittinger, K., Bushman, F.D., Costello, E.K., Fierer, N., Pena, A.G., Goodrich, J.K., Gordon, J.I., Huttley, G.A., Kelley, S.T., Knights, D., Koenig, J.E., Ley, R.E., Lozupone, C.A., McDonald, D., Muegge, B.D., Pirrung, M., Reeder, J., Sevinsky, J.R., Tumbaugh, P.J., Walters, W.A., Widmann, J., Yatsunenko, T., Zaneveld, J., Knight, R., 2010. QIIME allows analysis of high-throughput community sequencing data. Nat. Methods 7 (5), 335–336.

De Vrieze, J., Saunders, A.M., He, Y., Fang, J., Nielsen, P.H., Verstraete, W., Boon, N., 2015. Ammonia and temperature determine potential clustering in the anaerobic digestion microbiome. Water Res. 75, 312–323.

Deng, Y., Jiang, Y.-H., Yang, Y., He, Z., Luo, F., Zhou, J., 2012. Molecular ecological network analyses. BMC Bioinf. 13.

Duran, R., Bielen, A., Paradzik, T., Gassie, C., Pustijanac, E., Cagnon, C., Hamer, B., Vujaklija, D., 2015. Exploring Actinobacteria assemblages in coastal marine sediments under contrasted human influences in the West Istria Sea, Croatia. Environ. Sci. Pollut. Res. 22 (20), 15215–15229.

Edgar, R.C., Haas, B.J., Clemente, J.C., Quince, C., Knight, R., 2011. UCHIME improves sensitivity and speed of chimera detection. Bioinformatics 27 (16), 2194–2200.

Hart, S.C., Stark, J.M., Davidson, E.A., Firestone, M.K., 1994. Nitrogen mineralization, immobilization, and nitrification. In: Methods of Soil Analysis: Part 2—Microbiological and Biochemical Properties, pp. 985–1018.

Hatamoto, M., Kaneshige, M., Nakamura, A., Yamaguchi, T., 2014. *Bacteroides luti* sp. nov., an anaerobic, cellulolytic and xylanolytic bacterium isolated from methanogenic sludge. Int. J. Syst. Evol. Microbiol. 64, 1770–1774.

Hugoni, M., Taib, N., Debroas, D., Domaizon, I., Dufournel, I.J., Bronner, G., Salter, I., Agogue, H., Mary, I., Galand, P.E., 2013. Structure of the rare archaeal biosphere and seasonal dynamics of active ecotypes in surface coastal waters. Proc. Natl. Acad. Sci. USA 110 (15), 6004–6009.

Langille, M.G., Zaneveld, J., Caporaso, J.G., McDonald, D., Knights, D., Reyes, J.A., Clemente, J.C., Burkepile, D.E., Vega Thurber, R.L., Knight, R., Beiko, R.G., Huttenhower, C., 2013. Predictive functional profiling of microbial communities using 16S rRNA marker gene sequences. Nat. Biotechnol. 31 (9), 814–821.

Li, J.B., Rui, J.P., Pei, Z.J., Sun, X.R., Zhang, S.H., Yan, Z.Y., Wang, Y.P., Liu, X.F., Zheng, T., Li, X.Z., 2014a. Straw- and slurry-associated prokaryotic communities differ during co-fermentation of straw and swine manure. Appl. Microbiol. Biotechnol. 98 (10), 4771–4780.

Li, X., Rui, J., Mao, Y., Yannarell, A., Mackie, R., 2014b. Dynamics of the bacterial community structure in the rhizosphere of a maize cultivar. Soil Biol. Biochem. 68, 392–401.

Mao, C.L., Feng, Y.Z., Wang, X.J., Ren, G.X., 2015. Review on research achievements of biogas from anaerobic digestion. Renewable Sustainable Energy Rev. 45, 540–555.

Marisch, K., Bayer, K., Scharl, T., Mairhofer, J., Krempl, P.M., Hummel, K., Razzazi-Fazeli, E., Striedner, G., 2013. A comparative analysis of industrial *Escherichia coli* K-12 and B strains in high-glucose batch cultivations on process-, transcriptome- and proteome level. PLoS One 8 (8), 16.

Marti, R., Mieszkin, S., Solecki, O., Pourcher, A.M., Hervio-Heath, D., Gourmelon, M., 2011. Effect of oxygen and temperature on the dynamic of the dominant bacterial populations of pig manure and on the persistence of pig-associated genetic markers, assessed in river water microcosms. J. Appl. Microbiol. 111 (5), 1159–1175.

Maus, I., Cibis, K.G., Wibberg, D., Winkler, A., Stolze, Y., Konig, H., Puhler, A., Schluter, A., 2015. Complete genome sequence of the strain *Defluviitoga tunisiensis* L3, isolated from a thermophilic, production-scale biogas plant. J. Biotechnol. 203, 17–18.

Montoya, J.M., Sole, R.V., 2002. Small world patterns in food webs. J. Theor. Biol. 214 (3), 405–412.

Navarrete, A.A., Tsai, S.M., Mendes, L.W., Faust, K., de Hollander, M., Cassman, N.A., Raes, J., van Veen, J.A., Kuramae, E.E., 2015. Soil microbiome responses to the short-term effects of Amazonian deforestation. Mol. Ecol. 24 (10), 2433–2448.

Pap, B., Gyoerkei, A., Boboescu, I.Z., Nagy, I.K., Biro, T., Kondorosi, E., Maroti, G., 2015. Temperature-dependent transformation of biogas-producing microbial communities points to the increased importance of hydrogenotrophic methanogenesis under thermophilic operation. Bioresour. Technol. 177, 375–380.

Rui, J., Li, J., Zhang, S., Yan, X., Wang, Y., Li, X., 2015. The core populations and co-occurrence patterns of prokaryotic communities in household biogas digesters. Biotechnol. Biofuels 8, 158.

Salter, I., Galand, P.E., Fagervold, S.K., Lebaron, P., Obernosterer, I., Oliver, M.J., Suzuki, M.T., Tricoire, C., 2015. Seasonal dynamics of active SAR11 ecotypes in the oligotrophic Northwest Mediterranean Sea. ISME J. 9 (2), 347–360.

Tian, Z., Zhang, Y., Li, Y.Y., Chi, Y.Z., Yang, M., 2015. Rapid establishment of thermophilic anaerobic microbial community during the one-step startup of thermophilic anaerobic digestion from a mesophilic digester. Water Res. 69, 9–19.

Wallace, R.J., McKain, N., Broderick, G.A., Rode, L.M., Walker, N.D., Newbold, C.J., Kopecny, J., 1997. Peptidases of the rumen bacterium *Prevotella ruminicola*. Anaerobe 3 (1), 35–42.

Wang, Q., Garrity, G.M., Tiedje, J.M., Cole, J.R., 2007. Naive Bayesian classifier for rapid assignment of rRNA sequences into the new bacterial taxonomy. Appl. Environ. Microbiol. 73 (16), 5261–5267.

Weiland, P., 2010. Biogas production: current state and perspectives. Appl. Microbiol. Biotechnol. 85 (4), 849–860.

Weiss, S., Zankel, A., Lebuhn, M., Petrak, S., Somitsch, W., Guebitz, G.M., 2011. Investigation of microorganisms colonising activated zeolites during anaerobic biogas production from grass silage. Bioresour. Technol. 102 (6), 4353–4359.

Wilson, C.A., Murthy, S.M., Fang, Y., Novak, J.T., 2008. The effect of temperature on the performance and stability of thermophilic anaerobic digestion. Water Sci. Technol. 57 (2), 297–304.

Xu, S., He, C., Luo, L., Lu, F., He, P., Cui, L., 2015. Comparing activated carbon of different particle sizes on enhancing methane generation in upflow anaerobic digester. Bioresour. Technol. 196, 606–612.

Yamamoto, K., Hirao, K., Oshima, T., Aiba, H., Utsumi, R., Ishihama, A., 2005. Functional characterization in vitro of all two-component signal transduction systems from *Escherichia coli*. J. Biol. Chem. 280 (2), 1448–1456.

Yu, D., Kurola, J.M., Lahde, K., Kymalainen, M., Sinkkonen, A., Romantschuk, M., 2014. Biogas production and methanogenic archaeal community in mesophilic and thermophilic anaerobic co-digestion processes. J. Environ. Manage. 143, 54–60.

Zhang, Z.G., Geng, J.W., Tang, X.D., Fan, H., Xu, J.C., Wen, X.J., Ma, Z.S., Shi, P., 2014. Spatial heterogeneity and co-occurrence patterns of human mucosal-associated intestinal microbiota. ISME J. 8 (4), 881–893.

Zhang, W., Wang, Y., Bougouffa, S., Tian, R., Cao, H., Li, Y., Cai, L., Wong, Y.H., Zhang, G., Zhou, G., Zhang, X., Bajic, V.B., Al-Suwailem, A., Qian, P.-Y., 2015. Synchronized dynamics of bacterial niche-specific functions during biofilm development in a cold seep brine pool. Environ. Microbiol. 17 (10), 4089–4104.